Journal of Electron Spectroscopy and Related Phenomena 206 (2016) 18–23

Contents lists available at ScienceDirect

Journal of Electron Spectroscopy and Related Phenomena

journal homepage: www.elsevier.com/locate/elspec

Electronic and crystal structures of thermoelectric CaMgSi intermetallic compound

Hidetoshi Miyazaki[a,*], Manabu Inukai[a], Kazuo Soda[b], Nobufumi Miyazaki[c], Nozomu Adachi[c], Yoshikazu Todaka[c], Yoichi Nishino[a]

[a] Department of Frontier Materials, Nagoya Institute of Technology, Nagoya 466-8555, Japan
[b] Department of Quantum Engineering, Graduate School of Engineering, Nagoya University, Nagoya 464-8603, Japan
[c] Department of Mechanical Engineering, Toyohashi University of Technology, Toyohashi 441-8580, Japan

ARTICLE INFO

Article history:
Received 9 July 2015
Received in revised form 23 October 2015
Accepted 3 November 2015
Available online 10 November 2015

Keywords:
CaMgSi compound
Thermoelectric materials
Synchrotron radiation
Photoemission spectroscopy
X-ray powder diffraction

ABSTRACT

We investigated the electronic and crystal structures of a new thermoelectric material, CaMgSi compound, by using synchrotron radiation photoemission spectroscopy (SR-PES), synchrotron radiation X-ray powder diffraction (SR-XRD) measurements, and electronic band structure calculation to understand the way leading to improvement in the thermoelectric properties of this material. Electronic band structure calculation of the CaMgSi compound using the crystal structure determined from SR-XRD measurement showed a semi-metallic electronic structure with a pseudo-gap at the Fermi level. In contrast to the predicted semi-metallic electronic structure, the SR-PES results showed a small semiconductor-like gap at the Fermi level. This result revealed that the CaMgSi compound is a Mott-type insulator owing to strongly correlated electrons effect in the Ca 3*d* and Mg 3*p* states being well hybridized with those in the Si 3*p* states. The observed electronic structure of the CaMgSi compound suggests that an optimal carrier doping exists to best control the n- and p-type thermoelectric properties and enhance the power factors.

1. Introduction

Thermoelectric materials have attracted considerable attention as viable materials for direct conversion of thermal energy into electrical energy. In principle, the performance of thermoelectric materials is determined by their dimensionless figure of merit $ZT = S^2\sigma T/\kappa$, where S is the Seebeck coefficient, σ is the electrical conductivity, κ is the thermal conductivity, and T is the absolute temperature. Given this relation, high performance of n- and p-type thermoelectric materials should exhibit high Seebeck coefficients, large electrical conductivities, and low thermal conductivities.

Since Mg_2Si-based compounds do not include the rare-metal or heavy atoms and show high-performance of the thermoelectric properties, they are well- known candidates for thermoelectric materials with high economic performance and environmental harmonization [1–6]. Indeed, Mg_2Si-based compounds also have the lower density (1.88 g/cm^3) [2] compared to Bi–Te compounds (7.86 g/cm^3) [7], which are the conventional thermoelectric materials. Previous studies of n- and p-type thermoelectric properties of the Mg_2Si-based compounds have reported a ZT of 1.22 at 800 K and 0.11 at 873 K in $Mg_{2.10}Si_{0.49}Sn_{0.5}Sb_{0.01}$ [5] and $Mg_2SiAg_{0.01}$ [4] compounds, respectively. The lower p-type thermoelectric performance compared to the n-type one is a disadvantage of this otherwise promising material.

Recently, Todaka et al. investigated the thermoelectric properties of various Ca–Mg–Si compounds, in which one Mg atom in the Mg_2Si compound was substituted by a Ca atom, and suggested the existence of a CaMgSi phase with high p-type thermoelectric performance [8]. However, it is still unclear whether the high p-type thermoelectric property of the CaMgSi phase originates from composition deviation or the intrinsic electronic structure.

A band structure calculation predicts the stoichiometric CaMgSi compound to have a semi-metallic electronic structure with a narrow pseudo-gap of ~2.0 eV at the Fermi energy (E_F) [9]. In metallic systems, the S may be given a following formula [10]:

$$S(T) = \frac{\pi^2}{3}\frac{k_B^2}{-e}T\left(\frac{\partial \ln \sigma(E)}{\partial E}\right)_{E=E_F} \quad (1)$$

* Corresponding author. Tel.: +81 52 735 5394; fax: +81 52 735 5247.
E-mail address: miyazaki@nitech.ac.jp (H. Miyazaki).

http://dx.doi.org/10.1016/j.elspec.2015.11.002
0368-2048/

where $\sigma(E)$ denotes the electrical conductivity at a particular energy, E. Since $\sigma(E)$ is proportional to the density of states (DOS), $N(E)$, the above formula can be written as:

$$S(T) = \frac{\pi^2}{3}\frac{k_B^2}{-e}T\left(\frac{1}{N(E)}\frac{\partial N(E)}{\partial E}\right)_{E=E_F} \quad (2)$$

Large value of S arises from a low $N(E)$ coupled with a steep slope, $\partial N(E)/\partial E$, at E_F. Since the DOS rises sharply on both sides of the pseudo-gap, we expect the absolute value of S to be well enhanced and its sign to be controlled by carrier doping, such as off-stoichiometry or doping another element. Therefore, the CaMgSi compound with a pseudo-gap is one of extremely promising candidates for a next generation thermoelectric material.

Only a few studies have reported detailed crystal and electronic structures for the stoichiometric CaMgSi compound [9], despite the potential of this information suggests strategies to improve the thermoelectric properties. Synchrotron radiation powder diffraction (SR-XRD) and photoemission spectroscopy (SR-PES) have shown the detailed crystal and electronic structures. Hard X-ray photoemission spectroscopy (HAX-PES) with photoelectron emitted angle dependence returns information about the topmost surface layer and intrinsic bulk electronic structure [11]. Topmost surface layer property, such as surface oxide layer thickness, is important for p–n junctions in thermoelectric devices made with these materials because it is related to the electrical resistivity of the interface between the electrode and materials. Therefore, we performed high-resolution SR-XRD measurement to determine the detailed crystal structure of CaMgSi compound and SR-PES measurements at various excitation energies to investigate its electronic structure.

2. Experimental and theoretical procedures

A stoichiometric CaMgSi compound was fabricated by the powder metallurgical process. Mechanical ball-milling (MM) yielded finely pulverized and homogenized CaMgSi powders. Appropriate amounts of CaH_2 (99%, 200 μm), Mg (99.9%, <150 μm) and Si (99.9%, 5 μm) powders were mixed and milled in a planetary ball mill with a 500 ml capacity SUS304 pot and SUJ2 balls at Ar gas atmosphere. MM was performed at 125 rpm for 72 ks with 6×10^2 s rests every hour. A disk of CaMgSi compound was sintered from the prepared powderes by pulse-current sintering (PCS) process in a graphite mold at 1273 K for 1.2 ks in Ar gas and at 1273 K for 1.2 ks in vacuum under a uniaxial pressure of 50 MPa. Samples for SR-PES and SR-XRD measurements were cut from the disk with a SiC blade and they were again crushed to obtain a powder composed of particles with diameters smaller than 45 μm for SR-XRD measurement.

High-resolution SR-XRD measurement was carried out at 300 K using the BL02B2 beamline (wavelength $\lambda = 0.045993$ nm) at the SPring-8 synchrotron radiation facility in Japan [12]. The wavelength was precisely calibrated using a CeO_2 standard sample. A Rietveld analysis using the RIETAN-FP package [13] characterized the detailed crystal structure of the CaMgSi compound.

Electronic band structure of the CaMgSi compound was calculated with the WIEN2k package for full potential linearized augmented plane wave method and generalized gradient approximation [14]. The values determined from SR-XRD measurement were used as the CaMgSi compound lattice parameters. The convergence energy was set to 0.0001 Ry.

HAX-PES and soft X-ray PES (SX-PES) measurements were performed at the BL47XU [11] and BL27SU [15] beamlines of SPring-8, respectively. Clean surface for the HAX-PES measurement was obtained by *ex-situ* fracturing with a knife edge and immediately installing the sample in the HAX-PES chamber. Clean surface for the SX-PES measurement was obtained by *in-situ* fracturing with a knife edge at 10 K under an ultra-high vacuum. HAX-PES and SX-PES measurements were recorded at room temperature and 10 K, respectively. The Fermi level and total energy resolution were determined by the Fermi edge of evaporated gold films. The total energy resolutions of the HAX-PES and SX-PES measurements were set to 260 meV and 200 meV at the excitation photon energies ($h\nu$) of 7942 eV and 1000 eV, respectively.

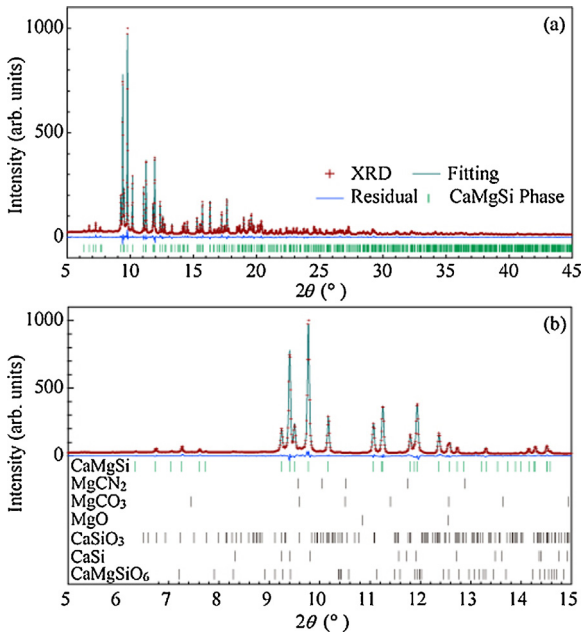

Fig. 1. Synchrotron radiation X-ray powder diffraction patterns (cross symbol) of wide (a) and narrow ranges (b) for CaMgSi compound at 300 K. The thin line, dots, and vertical bars indicate the fitting, residual, and CaMgSi phase results, respectively, calculated by Rietveld analysis. (For interpretation of the references to color in this figure legend, the reader is referred to the web version of this article.)

3. Results and discussion

Fig. 1 shows the SR-XRD pattern of the CaMgSi compound. Since several diffraction peaks could not be explained by the TiNiSi-type (Space group: No. 62) crystal structure, we performed a multi-phase analysis to determine other phases, such as oxides, carbides, and hydroxides, and their respective volume fractions. Table 1 shows the converged results of the SR-XRD pattern for the CaMgSi compound evaluated by the Rietveld analysis. The reliability factors, namely R_{wp}, R_p, R_e, and s, are sufficiently small to justify this fitting result.

Table 1
Reliability factors (R_{wp}, R_e and s), refined lattice parameter (a, b, c, α, β, and γ), isotropic displacement parameters (B), and occupancies determined for CaMgSi compound by Rietveld analysis.

R_{wp}	R_p	R_e	s
6.944	4.818	2.336	2.972

a (nm)	b (nm)	c (nm)	α (°)	β (°)	γ (°)
0.74666	0.44224	0.82958	90.0	90.0	90.0

Atom	Ca	Mg	Si
x	0.019	0.146	0.270
y	0.250	0.250	0.250
z	0.680	0.065	0.386
B (Å^2)	1.109	0.947	0.827
Occupancy	0.985	1.012	0.994